TEXTURE SEGMENTATION CONSIDERING MULTI BAND, MULTISCALE RESOLUTION AND AFFINE INVARIANT ROUGHNESS

ÉLDMAN DE OLIVEIRA NUNES, AURA CONCI

Instituto de Computação – UFF, R Passo da Pátria 156, 24210-240, Niterói, RJ, Brazil
eldman@bol.com.br , aconci@ic.uff.br,

Abstract. Texture segmentation is a basic task in the process of satellite image analysis. However, texture characterization is not an easy task specially when more than one wavelength band need to be considered. Several difficulties are present, as the basic texture definition in different resolution and image scales. Consequently, some approaches are essentially empiric and should be adjusted to different needs. This work presents a new method for combining multiband information for texture segmentation. It is based on an extension of fractal dimension analyze of texture for multi channel and is rotational invariant This method allow texture classification of thematic maps made from combination of N wavelength bands. The method was validated using mosaic of natural textures, comparison with others implementations and real satellite images.

1 Introduction

Textures image segmentation consists in identify image regions that are homogeneous with regard to some texture measure [10, 14, 17]. It is a topic greatly investigated in the last few years [1-4, 6-9, 11-13, 15, 19] and yet presenting several difficulties as the irregularity (in borders, brightness and shades) of natural textures [10]. It has many applications from industrial inspection and remote sensing to content-based image retrieval and biomedical image analysis. Several segmentation methods exists, but none is capable to segment all the types of images or consider important features like multi band, multi resolution and invariational aspect. Texture characterization is specially complex when more than only one wavelength band need to be considered, some works only combine texture on the usual RGB color bands [7,9,14,18]. Few approaches include rotational invariant possibilities but only for one band or gray-scale images [1,6,15]. Perhaps the characteristic more important in a segmentation method is the basic texture definition, the texton [16]. Mainly when the texton can appear in different resolution or scales. Wavelets and fractal based analysis presents adequate strategies to deal with multi scale representations [1-6,11-13,16]. Counting D-cubes or CDC is a technique to compute the local fractal dimension (FD) of N-dimensional images. This technique allows to calculate FD of thematic maps made from N wavelength bands [5]. This work presents a new kind of application for this technique. After the introduction of CDC method for multichannel images same experiments will be presented using it for multi band images segmentation. These experiments are designed to show the quality of texture segmentation using this tool and its scale and affine invariant characteristics.

2 Outline of the Method

This section presents the main aspect of the CDC technique [5], its possibilities and limitations as well as some particularities of conceptual approach. The main aspect of fractal geometry used in this application is the concept of fractal dimensions to characterize texture scaling behavior [2]. The word fractal refers to entities (in present study sets of pixels) that display a degree of self-similarity at different scales [11]. Although Hausdorff dimension is the main definition; for real images it is difficult implement algorithm for efficient estimation of this measure [4]. An alternative dimension in widespread use for a set A in Euclidean N-space is the box-counting or box dimension [16]. This provides a description of how much of the surface a set fills. If a set $A \in \Re^2$ is covered by just-touching boxes of side length $\varepsilon=(1/2)^n$ (figure 1), box dimension can be writing as

$$FD = \lim n \to \infty \, (\log N(A, \varepsilon)) / (\log 1/\varepsilon) \qquad (1)$$

where $N(A, \varepsilon)$ denotes the number of boxes of side length $\varepsilon=(½)^n$ which intersect the set A [5].

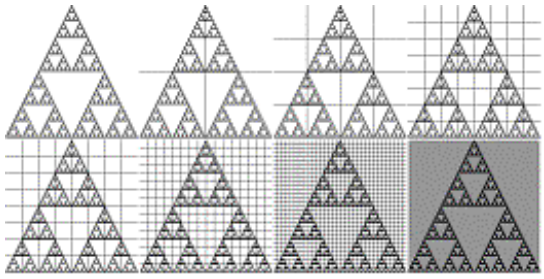

Figure 1 - Computing box dimension of Sierpinsky triangle (n = 0, 1, 2, 3, 4, 5, 6 and 7).

In algorithms for black & white set [15], the box dimension computation is processed in three steps. First, the image of ***MxM*** pixels is partitioned into grids of sxs pixels and scaled down to ***r=s/M*** (figure 1). Second, for each n the contributions from all grids ***N(A,ε)*** is computed. Then the limit in (1) is estimate from the least-squares linear fit of ***log N(A, ε) x log ε*** (figure 2).

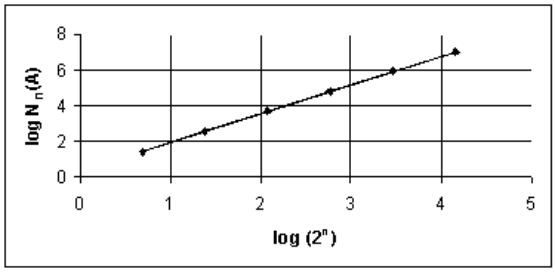

Figure 2 - Plotting ***log N(A, ε) x log ε*** for Sierpinsky triangle (figure 1) : FD ≈ 1.585.

A gray-scale image (or a band of multi banded image) fills all the underlined area [15]. There is not gaps, all spatial resolution pertains to the object and must be covered by boxes if equation (1) is used. Thus the box counting must be extended to consider the gray level. The image was now a 3D object (the third coordinate represent the pixel intensity), that is, it must be seen as an element of the space of functions [16].

$$f : \Re^2 \rightarrow G \qquad (2)$$

where ***G*** represents the set of intensity values of the image in a given band. Then a simple extension of box-counting to gray scale images is by the assumption that it is covered by three-dimensional box also in the image intensity direction. If ***G*** is the total number of gray levels then ***G/s'=M/s***. On each grid of ***MxM*** pixels image there is a column of boxes of size ***sxsxs'*** covering up to the maximum gray level of the grid, G_{max}. The box counting ***N(A, ε)*** for FD computation in equation (1) denotes the number of boxes of side length $\varepsilon=(1/2)^n$ which intercepted points of the set ***A***, also in the pixel intensity direction. The interception can be computed using the maximum and minimum pixel gray levels, G_{max} and G_{min} , of each box :

$$N(A, \varepsilon) = \sum \{ int [(G_{max} - G_{min}) / s'] + 1 \} \qquad (3)$$

and taking the contributions from all grids (Blanket Dimension [5]). Then, the expected range of FD for a gray level image (or an image band) is from 2 to 3.

Landsat-7 Thematic Mapper-TM sensors collect data from Blue to Red (Band 1: 0.54-0.52 μm, Band 2: 0.52-0.60 μm and Band 3: 0.63-0.69 μm) and beyond the Red end of the visible wavelength. There are three infrared bands: near-infrared (Band 4: 0.76-0.90 μm), mid-infrared (Band 5: 1.55-1.75 μm and Band 7: 2.08-2.35 μm) and there is a thermal infrared (Band 6: 10.4-12.5 μm). Figure 3 shows on grayscale bands 1 to 6 of the Landsat-7 image used in next section and also RGB fusion of bands 1, 2, 3 and 4, 5, 6 [7,18].

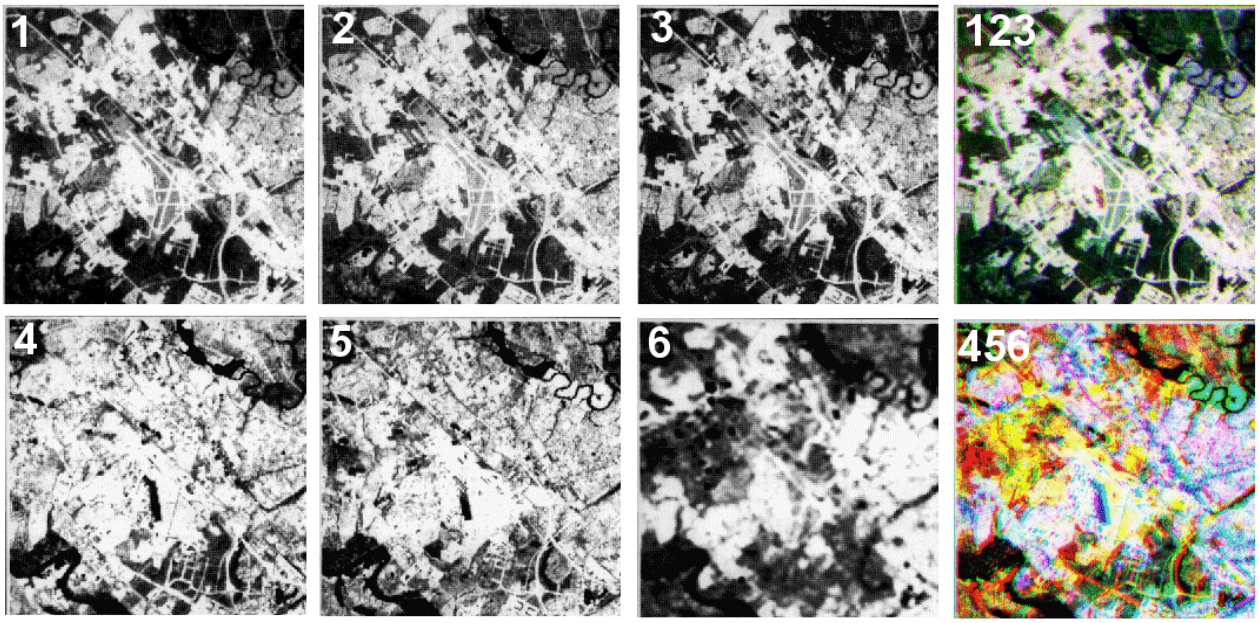

Figure 3 - Landsat-7 TM bands from a highly developed area with many highways from the U.S. east coast.

Approaches for determination of the FD of binary and monochrome images are modeled respectively in the 2-dimensional or 3-dimensional spaces. In synthesis, first they divide the plane ($\Re^2$) in squares or the space ($\Re^3$) in

cubes, then they compute the squares or cubes that intercept the binary or the gray level images respectively. Generalizing, we can suppose that the experimental determination of the FD of multi-channel images (in a multidimensional space $\Re^N$) implies in recursive division of the space in N-dimensional boxes followed by computation of those boxes intercepting the image. For conformity with previous works these N-dimensional boxes are named "N-boxes", where N identifies the dimension [16]. Thus, the 1-boxes are a line segment (one-dimensional), the 2-boxes are squares (two-dimensional), the 3-boxes are cubes (three-dimensional), the 4-boxes are four-dimensional cubes and N-boxes refers to N-dimensional cubes [5].

For black & white images, the 2D space is divided by identical parts of sides L_1xL_2 (2-boxes). L_1 and L_2 correspond to the axes of the image plane. For gray level images (or one band image), the space 3D is divided by identical parts of sides $L_1xL_2xL_3$ (3-boxes), where L_3 correspond at the intensity level of the image. For color images (or three bands) the space 5D is divided by parts of sides $L_1xL_2xL_3xL_4xL_5$ (5-boxes), where L_1 and L_2 are the image plane coordinates and L_3, L_4 and L_5 define the color in the considered color space (usually RGB).

For satellite images, according to the number, b, of considered bands, each axis in the ND space (N=b+2) is divided by the same number of parts resulting the N-boxes, in the N-dimensional space. So, each point in a color image needs 5 coordinates to be modeled. Points in satellite images need more components, depending on the number of used bands. To calculate the FD of Landsat-7, using all bands we needed to use 9 coordinates, that is each image pixel is a point of the 9 dimensional space.

Equation (1) must be extended for computing the N-boxes intersections with the image considering recursive subdivision of the ND space by ½. Observe that the number of box from recursive subdivision and its side length ε depend upon the space N dimension and the number of recursive divisions, d. For 2-boxes it can be determined by $\mathbf{2^{2.d}}$ and $(½.)^d$, respectively. For 3-boxes, they are $\mathbf{2^{3.d}}$, $(½.)^d$ where d is the number of half divisions. Generalizing, for 4-boxes, 5-boxes or N-boxes, the number of N-boxes of side length $\boldsymbol{\varepsilon}=(½.)^d$ is $\mathbf{2^{Nd}}$. For the determination of the N-dimensional FD, the interception of each channel with the image $\boldsymbol{A}$, $\boldsymbol{N(A, \varepsilon)}$ must be considered and used in expression (1).

3 Experiments

For CDC segmentation, textures are characterized by selecting image samples with 2x2, 4x4, 8x8, 16x16, 32x32 or 64x64 pixels. Such samples are used to define an tolerance criterion for DF feature association. After this supervised learning process the automatic segmentation process can initialized. This considers neighbors regions with FD variation (using all or the selected combination of bands) in the tolerance range as same texture. The user can define any number of texture classes to be identified and how their pixels are identify by the system as belonging to the class. For instance, on figure 13, five classes were specified using 4x4 samples, they are identified on the results using dark blue, light blue, red, orange and yellow.

We will not examine here the accuracy of the FD estimation for each channel or on classical fractal sets in black and white, because they have been treated in [5]. The experiments reported consider the new aspect of its uses in segmentation. For multi band or satellites images we don't know previous results considering all bands, so in order to verify the results, first we projected a series of testes where the results can be predict. These are the. invariance tests (on affine transformation and bands combination) projected in sections 3.1 to 3.3. to validated the approach. Then we compare this with others implementation (section 3.4). Finally in section 3.5 we tested our image segmentation algorithm on a real problem of remote sensing classification.

3.1 Invariance of DF on affine transformations

The method CDC measures textures characteristic of images based in they degree of FD computed considering all bands. Taking into account the characteristic of the human visual system (HSV), textured regions of an image with same visual impression must be invariant to rotations, translation, displacements and scale (all represented on affine transformations). CDC method extends these invariance concept for all the bands allowing find a texture, after affine transformations. Figure 4 shows some of the possible symmetries tested. The symmetries are obtained through the rotation and reflection of each pixel of the template. Figure 5 shows CDC invariance on resolution. The input image bands used are those on figure 3, using all image area a unique texture region.

3.2 Testing invariance band associations

Multispectral images can be visualized as color images if three bands are associated to the channels Red, Green and Blue. Each association of bands to RGB presets specific characteristics and applications. Adequate combination facilitates identification of areas through representation of the information in different colors. Conceptually, different ordination on combinations of same bands don't alter the complexity of the image. Thus, CDC results of FD should stay constant as shown in figure 6.

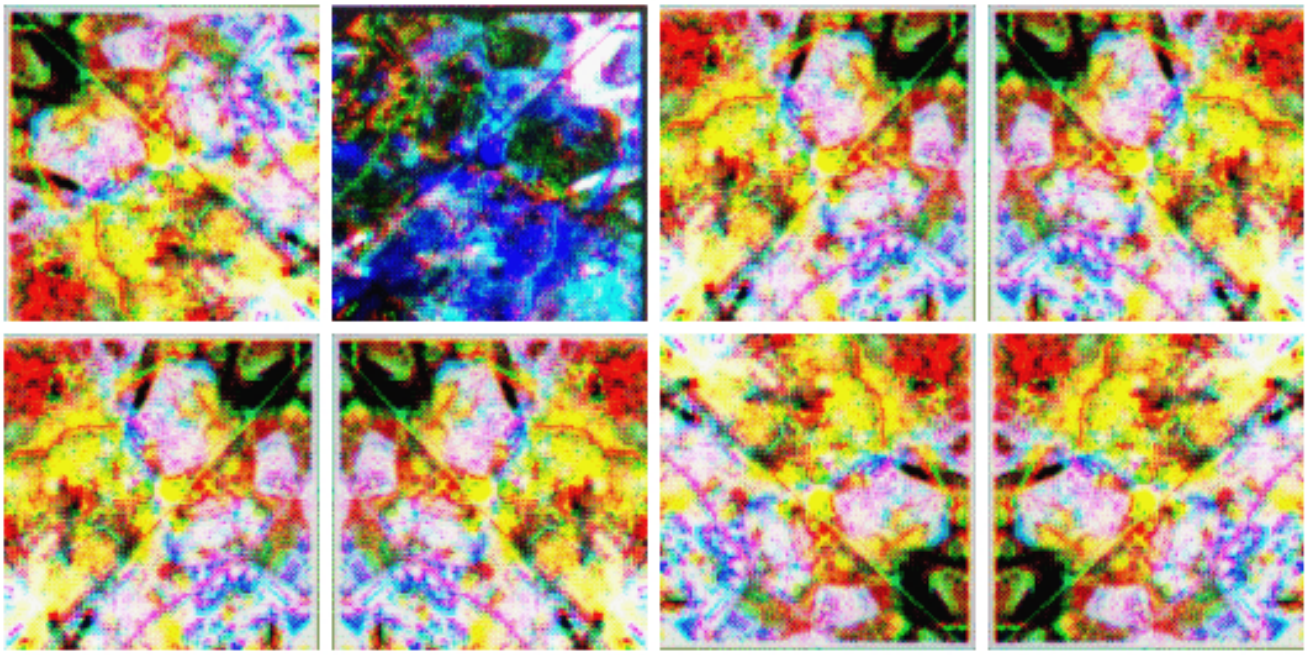

Figure 4 - Invariance (**FD ≈ 3.465**) on colors reflection (second image) and affine transformations.

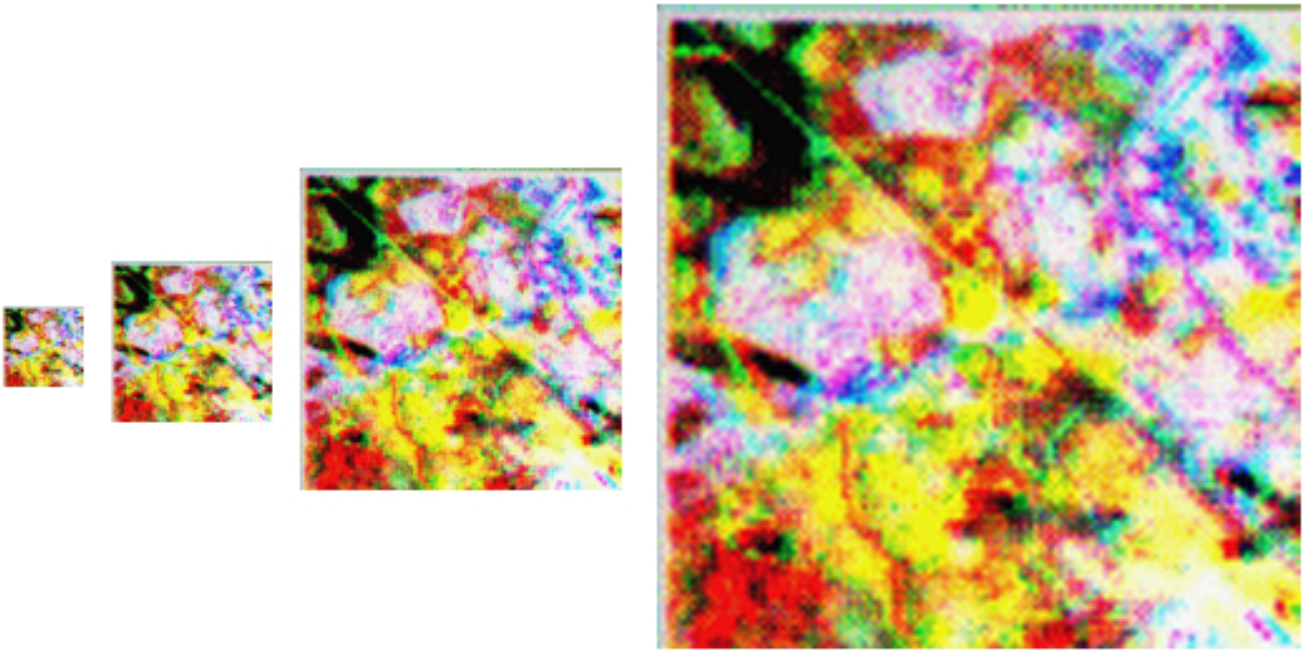

Figure 5 - CDC invariance (**FD ≈ 3.465**) on resolution

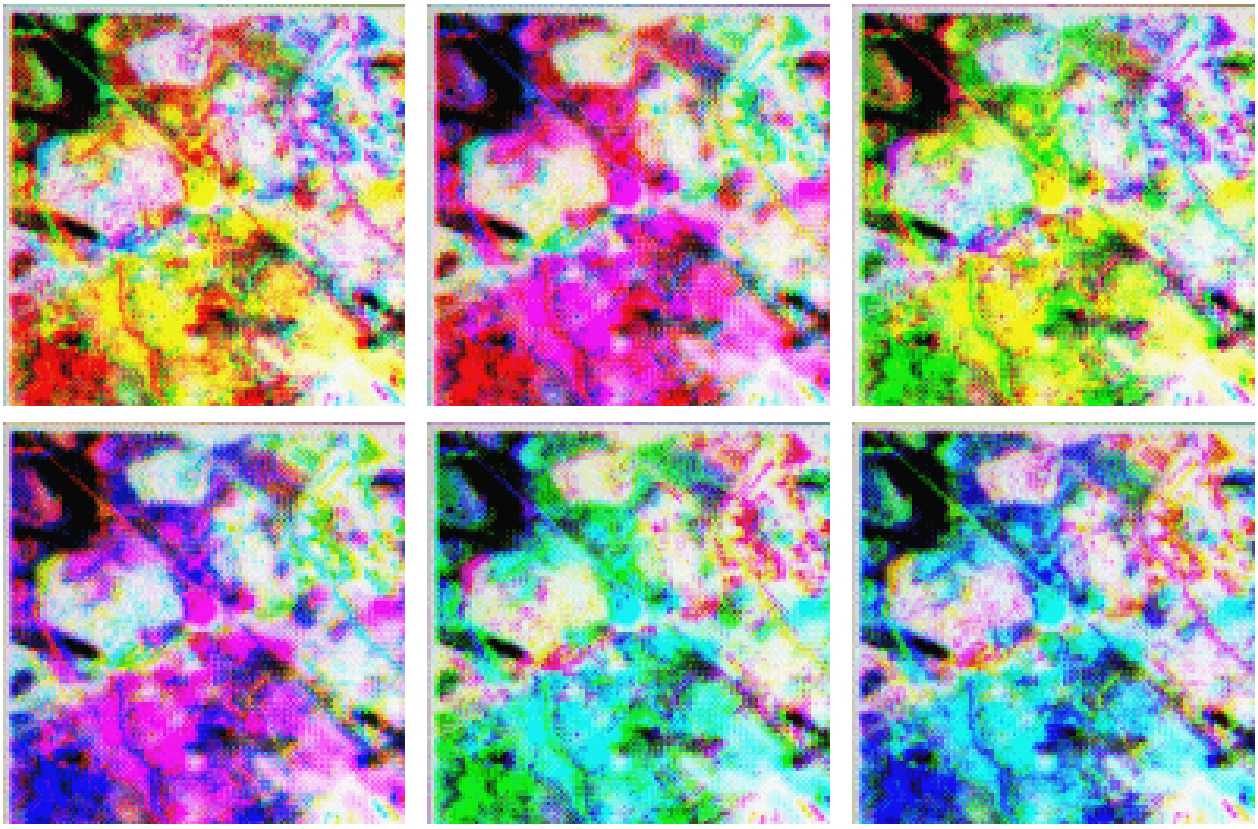

Figure 6 – CDC invariance (**FD ≈ 3.465**) on possible associations of the bands to the Channels RGB (4-5-6, 4-6-5, 5-4-6, 5-6-4, 6-4-5, 6-5-4.)

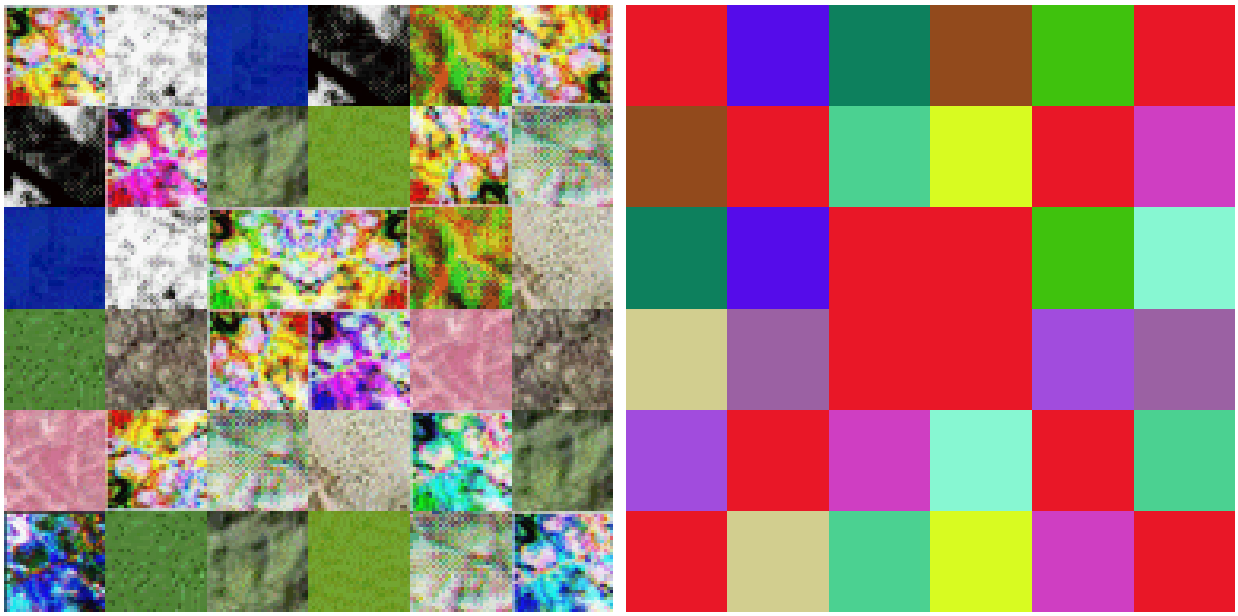

Figure 7 - Segmentation result: same color means same texture.

3.3 Segmentation test

A synthetic complex mosaic of natural texture (figure 7 left) made with patches of figure 3 and others natural textures from Landsat-7 TM was used to verify CDC method segmentation possibilities. Figure 7 (right) shows the areas were the method found similar FD with same colors along all figure. Although they are forced to appear with different color, because of the color RGB association used, comparing both images on figure 7 we can see that all regions with same fragments of textures are correctly found and merged (as the 12 patches used in 3.1 and 3.2).

3.4 Comparing segmentation results

In order to be used with other systems in this experimentation only the RGB channels are used. Figure 8 shows a mosaic of natural textures used for comparison with other implementations.

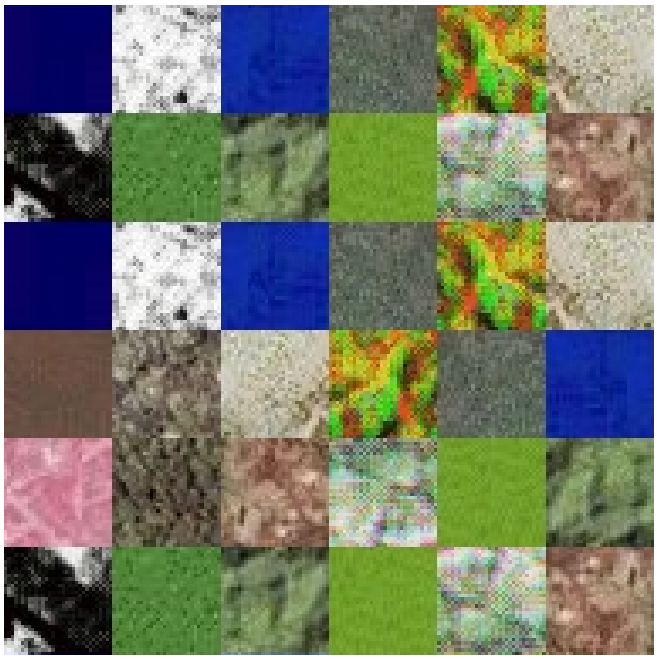

Figure 8 - Tested texture mosaic

Tree implementations for segmentation were used: SEGWIN, SPRING and the here proposed CDC. SEGWIN is based on region growth for analysis of the color and texture (http://www-iplab.ece.ucsb.edu/ segmentation/JSEG/). We can observe from figure 9 that there was a good differentiation of the textures in SEGWIN, but many bounds are not properly identified and two different textures are merged.

SPRING is based on area growth and statistical average among areas (http://www.inpe.br). Figure 10 presents the result of the segmentation of the images using SPRING. We can observe that there were an excellent definition of the contours and differentiation of the textures. However, due its unsupervised automatic classification some textures were subdivided in smaller areas losing its characteristics.

In figure 11 segmentation result using CDC is presented, now same textures are presented hatched with same color lines. Compare with figure 8, there is an excellent differentiation of the textures on CDC results.

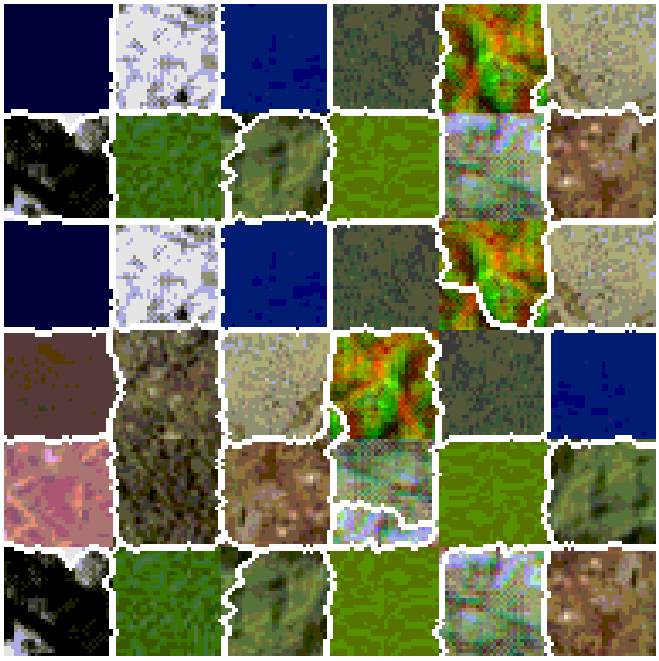

Figure 9 - Segmentation using SEGWIN.

3.5 Aerial image segmentation results

Figure 12 shows a satellite image from Patrocinio region (Minas Geraes - Brazil captured: 02-09-1999, 30m resolution by Landsat 5-TM). For this (from http: //www.engesat.com.br/download_imgs/downl_imgs. htm) color image 5-4-3 spectral band are combined to RGB. Different crops areas can clearly be identifies due to this combination, healthy vegetation emit more in the infrared band. Figure 13 shows the result of segmentation using the here proposed method. It accuracy identify the texture region ant their edge localization so quite high that we suggest a closed look of this results (use zoom on this figure).

4. CONCLUSIONS

A new idea is presented here: the use of multiband fractals for texture segmentation in image analysis. This is not a simple extension of the usual characterization of multifractal from its local dimension in gray-level images.

It is related to examine the interrelationship among the image representation in bands. Moreover, each band can be seen as a set in the 3D space, which means that its fractal dimension may present results between 2 and 3. Consequently, if two bands are considered in one gathering, their structure is a set in the 4D space and its fractal dimension may present results between 2 and 4. For multi-bands image the upper bound can be even larger. Experimes show that the method presented herein to handle the multi-band combination can be used on whatever combination of bands. It presents all expected invariational features of the human visual system (HSV), texture identifications are invariant to rotations, translation, scale, and also bands combination.

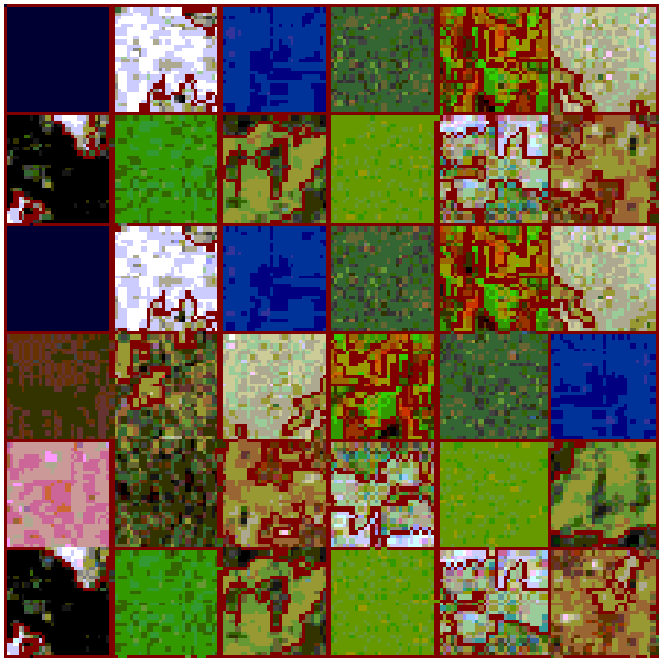

Figure 10 - Segmentation using SPRING.

5. REFERENCES

[1] D.Charalampidis, T. Kasparis, "Wavelet-Based Rotational Invariant Roughness Features for Texture Classification and Segmentation", IEEE Transaction on Image Processing, vol. 11 No. 8, August. 2002, pp-825-837.

[2] F. Camastra, A. Vinciarelli, "Estimating the intrinsic dimension of data with fractal-based methods", IEEE Transaction on Pattern Analysis and Machine Intelligence, Vol. 24, No. 10, October, 2002,1404-1407.

[3] P. Campisi, G. Scarano, "A multi resolution approach for texture synthesis using the circular harmonic functions", IEEE Transaction on Image Processing, vol. 11 No. 1, Jan. 2002, pp-37-51.

[4] A. Conci and L. H. Monteiro, "Multifractal Characterization of Texture Based Segmentation", Proceedings of IEEE International Conference on Image Processing, Vancouver, Canada, 1, 792-795 , 2000.

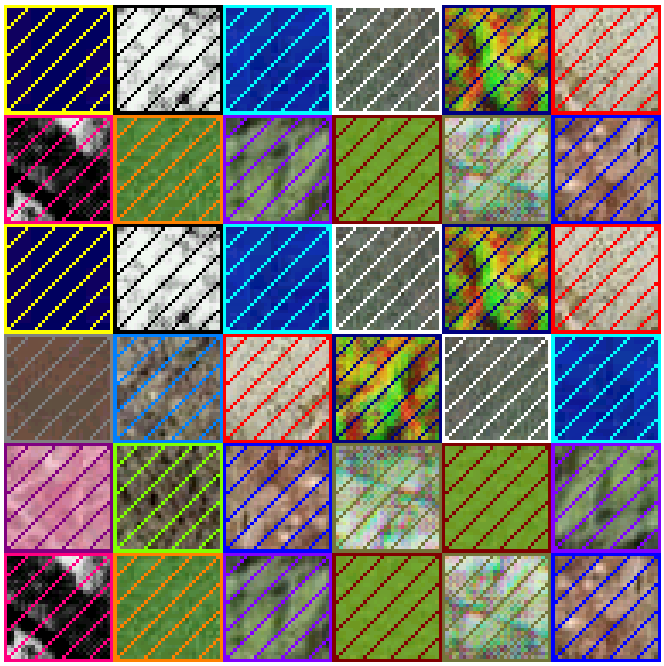

Figure 11 - Segmentation using CDC

Figure 12 – Region on the city of Patriocínio -MG (from Landsat 5-TM, 5-4-3 spectral band to RGB)

[5] A. Conci and E. O. Nunes "Multi-bands image analysis using local fractal dimension", proceedings of SIBGRAPI-Brazilian Symp. on Comp. Graphics, Image Proc.. and Vision, 91-99, 2001.

[6] M.N. Do, M. Vetterli, "Rotational invariant texture characterization and retrieval using steerable wavelet-domain hidden Markov Models", IEEE Transaction on Multimedia, Vol. 4, No. 4, December, 2002, 517-527.

[7] M.P. Dubuisson-Jolly, A. Gupta, "Color Texture fusion: application to aerial image segmentation and GIS updating", Image and Vision Computing, 18, 823-832, 2000.

[8] I. Epifanio, G. Ayala, "A random set view of texture classification", IEEE Transaction on Image Processing, vol. 11 No. 8, August. 2002, pp-859-867.

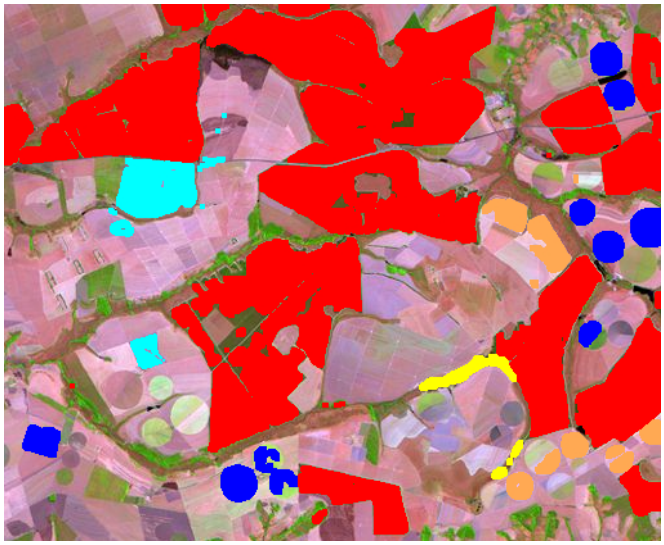

Figure 13 - Segmentation results by CDC

[9] T. Gevers, "Image Segmentation and Similarity of Color-Texture Objects", IEEE Transaction on Multimedia, Vol. 4, No. 4, December, 2002, 509-516.

[10] T. Gevers, "Adaptive Image Segmentation by Combining Photometry Invariant Region and Edge Information", IEEE Transaction on IEEE Transaction on Pattern Analysis and Machine Intelligence, Vol. 24, No. 6, Jun, 2002,848-852.

[11] L.M. Kaplan, "Extended fractal analysis for texture classification and segmentation", IEEE Transaction on Image Processing, vol. 8 No. 11, November. 1999, pp-1572-1585.

[12] T. Kasparis, D.Charalampidis, M. Georgiopoulous and J. Rolled, "Segmentation of textures images based on fractals and image filtering", Pattern Recognition, vol. 34. No. 1o, October. 2001, pp-1963-1973.

[13] K.I. Kim, K. Jung, S.H. Park, H.J. Kim, "Support Vector Machine for Texture Classification", IEEE Transaction on Pattern Analysis and Machine Intelligence, Vol. 24, No. 11, November,2002, 1542-1550.

[14] Mojsilocvic, J, Hu, E. Soljanin, "Extraction of perceptually important colors and similarity measurements for image matching retrieval and analysis" IEEE Transaction on Image Processing, vol. 11 No. 11, November. 2002, pp-1138-1248.

[15] T.Ojala, M. Pietikainen, T. Maenpaa, "Multi resolution gray-scale and rotation invariant texture classification with local binary patterns", IEEE Transaction on Pattern Analysis and Machine Intelligence, Vol. 24, No. 7, July,2002, 971-987.

[16] S. Peleg, J. Naor, R. Hartley and D. Avnir, "Multiple resolution texture analysis and classification", *IEEE Trans. Pattern Anal. Mach Intell.,* vol. 6, 518-523, 1984:

[17] T.R. Reed and H.J.M. du Buf, "A review of recent texture segmentation and feature extraction techniques", CVGIP: Image Understanding, vol. 57, No 3, pp. 359-372, 1993.

[18] D. A. Socolinsky, L. B. Wolff, "Multispectral Image Visualization through first-order fusion", IEEE Transaction on Image Processing, vol. 11 No. 8, August. 2002, pp-923-931.

[19] Stamos, "Geometry and Texture Recovery of Scenes of Large Scale", Computer Vision and Image Understanding, vol. 88, No. 2, November, 2002, 94-118.